# Self-Triggered Predictive Control of Nonlinear Systems Using **Approximation Model**

Lixing Yang, Samuel A. Dauchert, Xiaofeng Wang\*

Department of Electrical Engineering, University of South Carolina, Columbia, SC, 29208, USA

#### **SUMMARY**

This paper studies discrete-time model predictive control (MPC) of continuous-time nonlinear systems with measurement noises and exogenous disturbances. We consider the co-design of discrete-time finite horizon optimal control problem (FHOCP) and the associated self-triggering schemes that schedule the time instants for sampling the state and computing the FHOCP. The state-dependent nature of the selftriggered scheduling can not only dynamically adjust the inter-sampling period according to the system status, but dynamically discretize the model used in the FHOCP as well, in order to reduce the complexity of the FHOCP if designed appropriately. It is shown that the system can be stabilized with uniform ultimate boundedness, as long as the scheduling scheme matches the approximation model such that the one-step approximation error between the predicted state and the actual state is below a threshold related to the cost function. These results can be applied to most existing model approximation methods with either fixed or time-varying sampling rates. Copyright © 2015 John Wiley & Sons, Ltd.

Received ...

KEY WORDS: Self-Triggered Control, Model Predictive Control, Sampled-Data Systems

### 1. INTRODUCTION

Model predictive control (MPC) has been widely applied in many applications such as process control, power grids, transportation, robotics, and manufacturing, to name a few [1, 2]. It solves a finite horizon optimal control problem (FHOCP) at each sampling instant and applies a part of the optimal solution to the plant as the control inputs. When implemented in computers, the MPC algorithms are often in discrete-time, even though physical processes under control are usually continuous-time.

This motivates the research on sampled-data MPC, focusing on how to appropriately discretize the FHOCP and/or schedule the computation tasks of solving the FHOCPs. Early work studied periodic approaches, where sampling and solving the FHOCP, as well as discretizing the FHOCP, takes place in a periodic manner [3-11]. To make sure that the predicted states from solving the FHOCP are close to the actual states of the plant, the sampling period (or the upper bound on the sampling period) is usually very small. Such a selection could be very conservative with respect to computation efficiency. In general, solving an FHOCP is computationally expensive by itself, especially when it is nonlinear. A small sampling period implies frequently solving FHOCPs, which will generate a significant number of control tasks, which could place a heavy computational

Prepared using rncauth.cls [Version: 2010/03/27 v2.00]

<sup>\*</sup>Correspondence to: Department of Electrical Engineering, University of South Carolina, Columbia, SC, 29208, USA. Email: wangxi@cec.sc.edu

burden on the processor and introduce significant computation delays. Consequently, the system performance may be degraded and sometimes the system can even be unstable.

Consequently, aperiodic MPC was investigated including event-triggered and self-triggered MPC approaches. Event-triggered MPC solves the FHOCP when a pre-defined event occurs [12–21], while self-triggered MPC predicts the next the sampling instant in real-time [22–29]. In both approaches, the triggering time is related to not only the system dynamics but the current state/input information as well. Such an online determination mechanism allows the FHOCP to be solved in a less frequent manner and therefore saves computation resources.

It is worth pointing out, however, that all the previously mentioned work on aperiodic sampled-data MPC only focuses on when to solve the FHOCP, while leaving the FHOCP itself still continuous-time. Recently, a Lebesgue approximation based MPC approach was proposed in [30, 31] for nonlinear systems, where the sampling time and the state transitions in the approximation model are both aperiodic and state-dependent. It can enlarge the inter-sampling time intervals, while reducing the number of steps in the discrete-time FHOCP to prediction the same length of horizon in continuous-time domain. Therefore, both frequency and complexity of solving the FHOCP can be reduced. This result was extended later to stabilize nonlinear systems with measurement noises [32]. Both works are limited to first-order discrete-time approximation model in the FHOCP.

The contributions of this paper are listed as follows.

- We relax the assumption of first-order approximation in [30–32]. Our results are suitable to various model approximation methods with both periodic and aperiodic scheduling schemes.
- We present the mechanism to co-design the discrete-time FHOCP and the associated self-triggering algorithm. The self-triggering scheme is used to not only schedule the computation of the FHOCP, but determine the sampling period when discretizing the continuous-time plant model. Different from [30–32] where the scheduling schemes adopt very specific forms, the proposed self-triggering schemes can be quite flexible, which can potentially reduce the complexity of the FHOCP if designed appropriately, such as converting a complicated FHOCP into linear or convex programming.
- We develop sufficient conditions to guarantee feasibility and stability. It is shown that the discretized model in the FHOCP that approximates the plant only requires one-step accuracy, i.e., the approximation error between the predicted state and the real state at the next sampling instance (according to the self-triggering scheme) must be bounded by a threshold related to the cost function. This is an important condition that reveals the connection between the self-triggering law, the approximation model, and the cost function in the sampled-data MPC framework, to stabilize the system. Rigorous analysis on system stability is provided. We show that under these conditions, the states of the resulting closed-loop system will always stay inside a compact set and be uniformly ultimately bounded.
- We discuss the procedure to design parameters to meet the developed sufficient conditions.
   An illustrative example is presented to demonstrate the co-design procedure and the system performance. It shows that using the proposed method, nonlinear FHOCP can be converted into linear programming for a class of nonlinear systems, which can significantly save the computational resource.

The paper is structured as follows. The problem is formulated in Section 2 with the sampled-data MPC framework. Section 3 presents sufficient conditions for stability. Section 4 discusses the co-design guidelines with two illustrative examples in Section 5. Conclusions are discussed in Section 6. The proofs are presented in the appendix.

# 2. PROBLEM FORMULATION

**Notations**: We denote by  $\mathbb{R}^n$  the *n*-dimensional real vector space, by  $\mathbb{R}^+$  the set of real positive numbers, by  $\mathbb{R}^+_0$  the set of real nonnegative numbers, by  $\mathbb{Z}^+_0$  the set of nonnegative integers, and

by  $\mathbb N$  the set of natural numbers. We use  $\|\cdot\|$  to denote the Euclidean norm of a vector and the induced 2-norm of a matrix, and  $|\cdot|$  to denote the absolute value of a real number. Given a positive constant d, let  $\mathcal B(d)=\{x\in\mathbb R^n\mid \|x\|\leq d\}$ . Given two functions  $\alpha,\beta:\mathbb R\to\mathbb R$ ,  $\alpha\circ\beta(s)=\alpha(\beta(s))$ . Given two sets  $\mathcal X,\mathcal S\subseteq\mathbb R^n$ ,  $\mathcal X+\mathcal S$  is the Minkowski sum of these two sets. We use  $z^+=f(z)$  to represent the discrete-time system z(k+1)=f(z(k)). The symbols  $\mathbb I$  and e represent the identical matrix with appropriate dimensions and the Euler's number, respectively.

### Definition 2.1

A continuous function  $\alpha: \mathbb{R}_0^+ \to \mathbb{R}_0^+$  belongs to class  $\mathcal{K}$  if it is strictly increasing and  $\alpha(0) = 0$ .

### Definition 2.2

A set  $\mathcal{X}$  is called robust positively invariant (RPI) with respect to the system  $z^+ = f(z, w)$  and  $w \in \mathcal{W}$ , if for all  $w \in \mathcal{W}$  and for all  $z \in \mathcal{X}$ ,  $z^+ \in \mathcal{X}$  holds.

### Definition 2.3

The state x(t) of a system  $\dot{x} = f(x)$  is called uniformly ultimately bounded with ultimate bound b if there exist positive constants b and c, independent of  $t_0 \ge 0$ , and for every  $a \in (0,c)$ , there is  $T = T(a,b) \ge 0$ , independent of  $t_0$ , such that  $||x(t_0)|| \le a$  implies  $||x(t)|| \le b$  for any  $t \ge t_0 + T$ .

Consider a nonlinear continuous-time dynamical system:

$$\dot{x}(t) = f(x(t), u(t)) + v(t) 
x(t_0) = x_0$$
(1)

where  $x \in \mathbb{R}^n$  and  $u \in \mathcal{U}$  are the state and input of the system, respectively,  $\mathcal{U} \subseteq \mathbb{R}^m$  is the constraint set on the input including  $\{0\}$ ,  $v: \mathbb{R}^+ \to \mathbb{R}^n$  is the external disturbances,  $x_0 \in \mathbb{R}^n$  is the initial state, and  $f: \mathbb{R}^n \times \mathbb{R}^m \to \mathbb{R}^n$  is a continuous, locally Lipschitz function that describes the system dynamics satisfying f(0,0)=0. Assume that the disturbance v(t) is uniformly bounded by a positive constant  $d_v$ , i.e.,  $\|v(t)\| \leq d_v$  for all  $t \geq t_0$ .

### Remark 2.1

State constraints are not considered in this paper. We would like to point out, however, that the results in this paper can be easily extended to the case with the state constraints, following the approach in [31].

When implementing state-feedback MPC algorithms in digital environments, the controller receives measurements in discrete-time. The basic idea is described as follows: At the time instant  $t_k$ , the system samples the state and the controller obtains the sampled state  $\bar{x}(t_k)$ . Then the controller solves an N-step discrete-time FHOCP at time  $t_k$  with  $\bar{x}(t_k)$  as the initial condition. Let  $\{\hat{u}_k^{i,*}\}_{i=0}^{N-1}$  be the optimal control inputs of the FHOCP at  $t_k$ . Then  $\hat{u}_k^{0,*}$  will be actuated in the actual plant over the time interval  $[t_k, t_{k+1})$ , i.e.,  $u(t) = \hat{u}_k^{0,*}$  for any  $t \in [t_k, t_{k+1})$ . The next computation cycle starts at the time instant  $t_{k+1}$ .

Notice that the sampled state may contain measurement noises, i.e.,

$$\bar{x}(t_k) = x(t_k) + w(t_k) \tag{2}$$

where  $w : \mathbb{R} \to \mathbb{R}^n$  is the disturbance. So the measured initial state is  $\bar{x}_0 = x_0 + w(t_0)$ . Assume that the disturbance  $w(t_k)$  is bounded by a positive constant  $d_w$ , i.e.,  $||w(t_k)|| \le d_w$  for all  $k \in \mathbb{Z}_0^+$ .

### Remark 2.2

Although this paper considers state-feedback systems, the results can be extended to output-feedback systems, given an appropriately designed observer. In that case  $\bar{x}(t_k)$  can be regarded as an estimate of  $x(t_k)$  from the observer and  $w(t_k)$  then becomes the estimation error. The assumption of bounded measurement noises basically requires the estimation error to be uniformly bounded.

The discrete-time approximation model of the system in (1) is defined as follows. Suppose that at time  $t_k$  the controller receives the measurement  $\bar{x}(t_k)$ . The related approximation model then takes

the form as follows:

$$\hat{x}_k^{i+1} = \hat{f}(\hat{x}_k^i, \hat{u}_k^i) \tag{3a}$$

$$\hat{x}_k^0 = \bar{x}(t_k) \tag{3b}$$

where  $\hat{x}_k^i$  and  $\hat{u}_k^i$  are the predicted state and input at the ith state transition, respectively, and  $\hat{f}: \mathbb{R}^n \times \mathbb{R}^m \to \mathbb{R}^n$  is a continuous function.

Let  $N \in \mathbb{N}$  be the prediction horizon of the discrete-time FHOCP and the cost function is defined as follows:

$$J\left[\{\hat{u}_{k}^{i}\}_{i=0}^{N-1}|\bar{x}(t_{k})\right] = \sum_{i=0}^{N-1} \kappa(\hat{x}_{k}^{i}, \hat{u}_{k}^{i}) + V_{f}(\hat{x}_{k}^{N}),$$

where  $\kappa: \mathbb{R}^n \times \mathbb{R}^m \to \mathbb{R}_0^+$  is the running cost function and  $V_f: \mathbb{R}^n \to \mathbb{R}_0^+$  is the terminal cost function to be determined. Both  $\kappa$  and  $V_f$  must be locally Lipschitz and positive definite. Then the FHOCP at time  $t_k$  can be stated as follows:

$$V(\bar{x}(t_k)) = \min_{\hat{u}_k^i \in \mathcal{U}, \ i=0,\dots,N-1} J\left[\{\hat{u}_k^i\}_{i=0}^{N-1} | \bar{x}(t_k)\right]$$
 subject to equation (3a) and (3b), 
$$\hat{x}_k^N \in \mathcal{X}_{\mathcal{T}}, \tag{4}$$

where  $V:\mathbb{R}^n \to \mathbb{R}^+_0$  is the value function of the FHOCP and  $\mathcal{X}_{\mathcal{T}} \subseteq \mathbb{R}^n$  is the terminal set. Let  $\hat{u}_k^{i,*}, i=0,...,N-1$  be the optimal solutions to the FHOCP at  $t_k$  and  $\hat{x}_k^{i,*}$  be the corresponding optimal states. The next sampling time instant  $t_{k+1}$  can be defined as follows

$$t_{k+1} = t_k + \hat{g}(\hat{x}_k^{0,*}, \hat{u}_k^{0,*}) = t_k + \hat{g}(\bar{x}(t_k), \hat{u}_k^{0,*}), \tag{5}$$

where  $\hat{g}: \mathbb{R}^n \times \mathbb{R}^m \to \mathbb{R}^+$  is a positive function that must be strictly greater than zero, and

$$u(t) = \hat{u}_k^{0,*}, \quad [t_k, t_{k+1}).$$

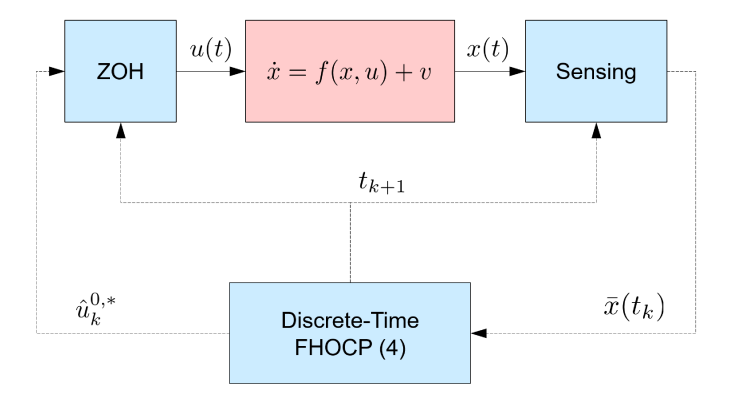


Figure 1. The closed-loop system diagram. The continuous-time plant is controlled by a discrete-time MPC controller with a self-triggered sampling scheme.

The overall MPC algorithm is summarized in Figure 1. At time  $t = t_k$ , the controller will

- (i) Sample the state and obtain  $\bar{x}(t_k)$ ;
- (ii) Solve the FHOCP in equation (4) for  $\hat{x}_k^{i,*}$  and  $\hat{u}_k^{i,*}$ ;

- (iii) Set  $t_{k+1}$  using equation (5);
- (iv) Send the optimal solution  $\hat{u}_k^{0,*}$  to the plant, i.e., set  $u(t) = \hat{u}_k^{0,*}$  over  $[t_k, t_{k+1})$ ; and
- (v) Start the next computation cycle at time  $t_{k+1}$ .

Under this framework, we will develop the conditions on the functions  $\hat{f}$ ,  $\hat{g}$ ,  $\kappa$ ,  $V_f$ , and  $\mathcal{X}_T$  that can guarantee stability of the closed-loop system defined by (1) – (5) subject to the input constraint, i.e.,  $u(t) \in \mathcal{U}$  for all  $t \geq t_0$ .

### 3. STABILITY CONDITIONS

This section presents the conditions on the parameters in the sampled-data MPC framework with the goal of stabilizing the system in (1). In the discussion we intend to leave  $\hat{f}$  and  $\hat{g}$  as general as possible, so that the results can be flexible to different model approximation approaches. We start from defining the terminal set  $\mathcal{X}_{\mathcal{T}}$ .

# Assumption 3.1

There exist a positive constant  $d_{\tilde{x}}$  and a feedback law  $h: \mathbb{R}^n \to \mathbb{R}^m$  satisfying h(0) = 0, such that the RPI set of the system  $z^+ = \hat{f}(z + \tilde{x}, h(z + \tilde{x}))$  exists with  $\tilde{x} \in \mathcal{B}(d_{\tilde{x}}) \subset \mathbb{R}^n$ .

With Assumption 3.1,  $\mathcal{X}_{\mathcal{T}}$  can be defined as this RPI set.

Let  $d_0$  be a large enough positive constant and

$$\mathcal{V}_0 = \{ x \in \mathbb{R}^n \mid V(x) \le d_0 \} \tag{6}$$

where V(x) is defined in (4). Then we introduce the following assumptions, which actually place requirements on the parameters in the FHOCP.

### Assumption 3.2

There exist class K functions  $\alpha_1$ ,  $\alpha_2$ ,  $\beta_1$ , and  $\beta_2$  such that

$$\kappa(x, u) \ge \alpha_1(\|x\|), \ \forall x \in \mathcal{V}_0, \ \forall u \in \mathcal{U},$$
 (7)

$$V(x) \le \alpha_2(\|x\|), \ \forall x \in \mathcal{V}_0 \tag{8}$$

$$\beta_1(\|x\|) \le V_f(x) \le \beta_2(\|x\|), \ \forall x \in \mathbb{R}^n$$

hold.

Let  $d_x$  be a positive constant that satisfies

$$d_x > \alpha_1^{-1}(d_0) + d_w$$

and  $\mathcal{X}_{\hat{f}}$  be the N-step reachable set of the system  $z^+ = \hat{f}(z,u)$  with the initial state  $z(0) \in \mathcal{B}(d_x + d_w)$  and  $u \in \mathcal{U}$ . Notice that because  $\hat{f}$  is continuous and  $\mathcal{U}$ ,  $\mathcal{B}(d_x + d_w)$  are compact,  $\mathcal{X}_{\hat{f}}$  must be compact.

### Assumption 3.3

There exist positive constants  $L_{\hat{f}}$ ,  $L_{\kappa}$ ,  $L_{V_f}$ ,  $L_f$ , and  $L_u$  such that for any  $x_1, x_2 \in \mathcal{X}_{\hat{f}}$  and  $u \in \mathcal{U}$ ,

$$\|\hat{f}(x_1, u) - \hat{f}(x_2, u)\| \le L_{\hat{f}} \|x_1 - x_2\| \tag{10}$$

$$\|\kappa(x_1, u) - \kappa(x_2, u)\| \le L_{\kappa} \|x_1 - x_2\| \tag{11}$$

$$||V_f(x_1) - V_f(x_2)|| \le L_{V_f} ||x_1 - x_2|| \tag{12}$$

and for any  $x \in \mathcal{B}(d_x)$  and  $u \in \mathcal{U}$ ,

$$||f(x,u) - f(0,0)|| \le L_f ||x|| + L_u ||u|| \tag{13}$$

hold.

Given a pair  $(\bar{x}, u) \in \mathcal{V}_0 \times \mathcal{U}$ , let z(t) be the solution to  $\dot{z}(t) = f(z(t), u) + v(t)$  with  $z(0) = \bar{x} + w$  and  $w \in \mathcal{B}(d_w)$ . Based on Assumption 3.3, z(t) admits a unique solution. Then there always exists a function  $\epsilon(\bar{x}, u)$  such that for any  $||v(t)|| \leq d_v$ , the following inequality

$$||z(\hat{g}(\bar{x},u)) - \hat{f}(\bar{x},u)|| \le \epsilon(\bar{x},u) \tag{14}$$

holds. Back to our framework, this inequality actually indicates a state/input-dependent bound on the difference between the actual state  $x(t_{k+1})$  and the first predicted state  $\hat{x}_k^1$  generated by the discrete-time approximation model in (3), i.e.,  $\|x(t_{k+1}) - \hat{x}_k^1\| \leq \epsilon(\bar{x}(t_k), u(t_k))$ . Then

$$\epsilon_{\max} = \max_{x \in \mathcal{V}_0, \ u \in \mathcal{U}} \epsilon(x, u) \tag{15}$$

is actually a constant upper bound on the approximation error.

### Remark 3.1

In practice, finding the optimal solution in (15) might be computationally expensive. Instead, we just need an upper bound on  $\epsilon(x, u)$  over  $x \in \mathcal{V}_0$  and  $u \in \mathcal{U}$ , which will be much easier to calculate.

### Assumption 3.4

For any  $x \in \mathcal{X}_{\mathcal{T}} + \mathcal{B}\left((d_w + \epsilon_{\max})L_{\hat{f}}^{N-1}\right)$ , the function h(x) satisfies

$$h(x) \in \mathcal{U}$$
, and (16)

$$V_f\left(\hat{f}(x,h(x))\right) - V_f(x) \le -\kappa(x,h(x)) \tag{17}$$

hold.

### Remark 3.2

This is a standard assumption in MPC formulation except that equations (16) and (17) must be valid over a slightly larger set other than the terminal set  $\mathcal{X}_{\mathcal{T}}$  due to system disturbances, measurement noises, and modeling error in the FHOCP.

# Assumption 3.5

There exist two positive constants  $\rho \in (0,1)$  and d such that for any  $x \in \mathcal{V}_0$  and  $u \in \mathcal{U}$ ,

$$\theta \epsilon(x, u) < \rho \kappa(x, u) + d,$$
 (18)

where

$$\theta = \sum_{i=1}^{N-1} L_{\kappa} L_{\hat{f}}^{i-1} + L_{V_f} L_{\hat{f}}^{N-1}.$$
 (19)

### Remark 3.3

Assumption 3.5 places a threshold on the function  $\epsilon(x,u)$  that measures the model approximation error. In fact, this assumption, together with inequality (14), establishes a relation between the discrete-time approximation model (characterized by  $\hat{f}$ ), the self-triggering scheme (characterized by  $\hat{g}$ ), and the running cost (characterized by  $\kappa$ ). It indicates that, although  $\hat{f}$  and  $\hat{g}$  can be designed in different ways, the resulting approximation error must be bounded by a threshold related to the running cost function.

# Theorem 3.1

Consider the system in (1) with the controller defined in (4). Suppose that Assumption 3.1–3.5 hold. If the FHOCP is feasible at  $t_0$  with  $\bar{x}(t_0) \in \mathcal{V}_0$  and the following inequalities

$$t_{k+1} - t_k \le T_{\max}(d_x), \quad \forall k \in \mathbb{Z}_0^+, \tag{20}$$

$$d_{\tilde{x}} \ge (d_w + \epsilon_{\max}) L_{\hat{f}}^{N-1},\tag{21}$$

$$d_0 - d_w \theta - d \ge \max_{\alpha_1(\|x\|) \le \frac{d_w \theta + d}{1 - \rho}} \left[ V(x) - (1 - \rho) \alpha_1(\|x\|) \right]$$
(22)

hold, where

$$T_{\max}(d_x) = \frac{\log\left(1 + \frac{L_f(d_x - d_w - \alpha_1^{-1}(d_0))}{L_f(\alpha_1^{-1}(d_0) + d_w) + L_u \max_{u \in \mathcal{U}} \|u\| + d_v}\right)}{L_f}$$
(23)

then  $\bar{x}(t_k) \in \mathcal{V}_0$  for all  $k \in \mathbb{Z}_0^+$ ,  $x(t) \in \mathcal{B}(d_x)$  for all  $t \geq t_0$ , and the closed-loop system is uniformly ultimately bounded.

### Remark 3.4

Inequality (20) places an upper bound on the inter-sampling time intervals for safety reason. This ensures that x(t) will not deviate too much from  $\bar{x}(t_k)$  over  $[t_k, t_{k+1})$ . According to Theorem 3.1, it guarantees that x(t) stays inside  $\mathcal{B}(d_x)$ . Based on the definition of  $T_{\max}(d_x)$ , it can be arbitrarily large by simply increasing  $d_x$  in linear systems. For highly nonlinear systems, however, large  $d_x$  might result in large  $L_f$  and  $L_u$ . In that case there may exist an upper bound on  $T_{\max}(d_x)$ , due to the limitation of system dynamics. Moreover, large  $d_x$  and  $d_0$  may lead to large  $\epsilon_{\max}$  and therefore cause issues on the existence of h(x) satisfying (16) and (17).

### Remark 3.5

Inequality (21) means that the terminal set  $\mathcal{X}_{\mathcal{T}}$  must be able to guarantee set invariance in the presence of disturbances with the maximum magnitude of  $(d_w + \epsilon_{\max})L_f^{N-1}$ , while  $(d_w + \epsilon_{\max})L_f^{N-1}$  is actually an upper bound on the accumulated prediction error after N steps.

### Remark 3.6

Inequality (22) is used to ensure that the ultimate set (characterized by  $\frac{d_w\theta+d}{1-\rho}$ ) for  $\bar{x}(t_k)$  is included in  $\mathcal{V}_0$  such that the behavior of  $\bar{x}(t_k)$  can be limited inside  $\mathcal{V}_0$ . When  $d_v=d_w=d=0$ , inequality (22) can be removed, since in that case  $V(\bar{x}(t_{k+1})) \leq V(\bar{x}(t_k)) \leq \cdots \leq V(\bar{x}(t_0)) \leq d_0$  will always hold.

### 4. PARAMETER DESIGN

This section discusses how to co-design of the FHOCP and the scheduling function  $\hat{g}$  to meet the stability conditions. One of the challenges is that it may be hard to find the function V(x) and therefore the elements in the set  $\mathcal{V}_0$  cannot be explicitly identified. Alternatively, in the design procedure we usually choose  $\kappa(x,u)$  that satisfies (7) for any  $x \in \mathbb{R}^n$  and any  $u \in \mathcal{U}$ . Then we know that for any  $x \in \mathbb{R}^n$ ,

$$V(x) > \kappa(x, \hat{u}^*) > \alpha_1(\|x\|)$$
 (24)

holds, where  $\hat{u}_*$  is the first element of the optimal control inputs to the FHOCP with the initial state x. With this inequality, we can define the set  $\mathcal{X}_0$  as follows:

$$\mathcal{X}_0 = \{ x \in \mathbb{R}^n \mid \alpha_1(\|x\|) \le d_0 \}$$
 (25)

and obviously  $V_0 \subseteq \mathcal{X}_0$ . As a result, the assumptions in Theorem 3.1 can be verified over  $\mathcal{X}_0$ . For instance, if there exist an upper bound on V(x) over  $\mathcal{X}_0$ , inequality (8) in Assumption 3.2 can always be satisfied [33].

Most model approximation methods [34] or numerical approaches admit explicit forms of  $\epsilon(x, u)$  in inequality (14). For instance, Euler forward method has the following iteration

$$\hat{x}_k^{i+1} = \hat{f}(\hat{x}_k^i, \hat{u}_k^i) = \hat{x}_k^i + Tf(\hat{x}_k^i, \hat{u}_k^i)$$

where T is the sampling period. It is a first-order approximation with the truncation error  $\mathcal{O}(T^2)$ . Traditional approaches with higher-order truncation error include midpoint method  $(\mathcal{O}(T^3))$ , Heun's

method  $(\mathcal{O}(T^3))$ , Runge-Kutta method  $(\mathcal{O}(T^5))$ , and explicit Runge-Kutta method, to name a few. All these approximation models can be used in our framework as the discrete-time approximation model. The approximation error bound in these approaches, i.e.,  $\epsilon(x,u)$ , usually can be arbitrarily small by reducing the sampling period T. As an extension in our framework, T can be time-varying, dependent of  $\bar{x}(t_k)$  or  $(\hat{x}_k^i, \hat{u}_k^i)$  to cancel certain nonlinearity in  $\hat{f}$  from  $f(\hat{x}_k^i, \hat{u}_k^i)$ , such as

$$\hat{x}_{k}^{i+1} = \hat{x}_{k}^{i} + \hat{g}(\hat{x}_{k}^{i}, \hat{u}_{k}^{i}) f(\hat{x}_{k}^{i}, \hat{u}_{k}^{i})$$

using Euler method. In either case, the sampling period must be chosen in a way that the resulting approximation error satisfies inequality (18). To do so, one can choose  $\hat{g}$  first to simplify the structure of  $\hat{f}$  if possible and then identify  $\kappa$  that meets (18), or inversely, pick  $\kappa$  first and then select  $\hat{g}$  small enough such that inequality (18) holds. Notice that there may be many ways to choose  $\hat{g}(x,u)$ . We must guarantee the existence of a positive lower bound on  $\hat{g}(x,u)$  for any  $x \in \mathcal{X}_0/\{0\}$  and  $u \in \mathcal{U}/\{0\}$  to avoid Zeno behavior.

The parameters h and  $\mathcal{X}_{\mathcal{T}}$  must be defined together to meet Assumption 3.1 and 3.4. For linear systems, one can use the MPT toolbox [35] to compute the maximum RPI set inside  $\{x \in \mathbb{R}^n \mid h(x) \in \mathcal{U}\}$ . For nonlinear systems, we can consider input-to-state stability of the system

$$z^{+} = \hat{f}(z + \tilde{x}, h(z + \tilde{x})),$$

and design the feedback law h(z) such that

$$V_f(z^+) - V_f(z) \le -\kappa(z, h(z)) + \gamma(\|\tilde{x}\|)$$

holds for all  $z \in \mathcal{X}_0$  and  $\tilde{x} \in \mathcal{B}(d_{\tilde{x}})$ , where  $\gamma$  is a class  $\mathcal{K}$  function. Obviously, when  $\tilde{x} \equiv 0$ , inequality (17) is recovered. Since  $\|\tilde{x}\| \leq d_{\tilde{x}}$ , we have

$$V_f(z^+) - V_f(z) \le -\alpha_1(||z||) + \gamma(d_{\tilde{x}}).$$

With inequality (9), we know that the set

$$\left\{ x \in \mathbb{R}^n \mid V_f(x) \le \max_{s \in \left[0, \alpha_1^{-1} \circ \gamma(d_{\bar{x}})\right]} (\beta_2 - \alpha_1)(s) + \gamma(d_{\bar{x}}) \right\}$$
 (26)

is a RPI set that meets Assumption 3.1. Then we can reduce the size of  $d_{\tilde{x}}$  such that  $\mathcal{X}_{\mathcal{T}}$  is small enough to guarantee inequality (16).

# 5. ILLUSTRATIVE EXAMPLES

This section presents two examples to demonstrate how the theoretical results can be applied to co-design the FHOCP and the scheduling scheme.

# 5.1. Example 1

The nonlinear system under consideration is as follows:

$$\dot{x}_1 = \frac{(0.2e^{0.1(x_1+x_2)} + 1)(0.5x_1 + 5x_2)}{0.5x_1\sin(x_1) + 2} + v_1(t)$$

$$\dot{x}_2 = \frac{(0.2e^{0.1(x_1+x_2)} + 1)(2.5x_1 + 1.25x_2 + 2u)}{0.5x_1\sin(x_1) + 2} + v_2(t).$$

Assume that  $d_v = 10^{-4}$ ,  $d_w = 10^{-5}$ , and the input constraint is  $|u(t)| \le 2$ .

Let N=4 and the set  $\mathcal{X}_0$  defined by

$$\mathcal{X}_0 = \{ \bar{x} \in \mathbb{R}^n \mid ||\bar{x}|| \le 1 \}.$$

Let  $d_x = 1.15$ . Then  $L_f = 3.4561$ ,  $L_u = 1.2246$  over  $x \in \mathcal{B}(d_x)$  and  $T_{\max}(d_x) = 0.0243$ .

Using Euler-forward method to approximate this nonlinear system, we obtain the approximation model

$$\begin{split} \hat{x}_k^{i+1} &= \hat{f}(\hat{x}_k^i, \hat{u}_k^i) \\ &= \hat{x}_k^i + \hat{g}(\hat{x}_k) f(\hat{x}_k, u_k^i) \\ &= \underbrace{\left( \underbrace{1 + \underbrace{\left( \begin{array}{c} 0.005 & 0.05 \\ 0.025 & 0.0125 \end{array} \right)}_{A} \right)}_{i} \hat{x}_k^i + \underbrace{\left( \begin{array}{c} 0 \\ 0.02 \end{array} \right)}_{B} \hat{u}_k^i \end{split}$$

where

$$\hat{g}(x) = \frac{0.005x_1\sin(x_1) + 0.02}{0.2e^{0.1(x_1 + x_2)} + 1}.$$
(27)

Notice that with the state-dependent  $\hat{g}$ , the model used in the FHOCP becomes linear.

Given the set  $\mathcal{X}_0$ , we can see that  $\hat{g}_{\max} = \max_{x \in \mathcal{X}_0} \hat{g}(x) = 0.0205 < T_{\max}(d_x)$ . So inequality (20) is trivially satisfied. Given the approximation model  $\hat{f}$ , we can calculate the approximation error bound  $\epsilon(x,u)$  on  $||z(\hat{g}(x)) - \hat{f}(x,u)||$ :

$$\epsilon(x,u) = \left(\hat{g}(x)\|f(x,u)\| + \frac{d_v}{L_f} + d_w\right) \left(e^{L_f \hat{g}(x)} - 1\right) + d_w$$
$$= \left(\|Ax + Bu\| + \frac{d_v}{L_f} + d_w\right) \left(e^{L_f \hat{g}(x)} - 1\right) + d_w.$$

Notice that this bound  $\epsilon$  is valid for any positive function  $\hat{g}$ . Now we apply the definition of  $\hat{g}$  in (27) into the equation above and define the cost function to guarantee inequality (18). Let  $\rho = 0.6225$ ,  $\theta = 12.8132$ ,

$$\kappa(x, u) = 0.08||x|| + 0.0302||u||, V_f(x) = ||Px||,$$

$$P = \begin{pmatrix} -2.7502 & -5.9069 \\ -9.0017 & -3.5196 \end{pmatrix}, K = (-5.9346 - 5.4436),$$

$$d = \left(\left(\frac{d_v}{L_f} + d_w\right) \left(e^{L_f \hat{g}_{\text{max}}} - 1\right) + d_w\right) \theta = 1.6476 \times 10^{-4},$$

 $L_{\kappa}=0.08,\ L_{V_f}=10.9602,\ {\rm and}\ \epsilon_{\rm max}=0.0053.$  The parameters P and K are computed using the technique proposed in [36], such that inequality (17) holds with h(x)=Kx. With such a setting, the FHOCP becomes linear programming and the explicit solution can be found to speed up the computation [37]. Of course, in many cases, it is infeasible to convert the FHOCP to as simple as linear programming. However, by appropriately choosing  $\hat{g}$ , it is still possible to simplify the FHOCP, such as transforming nonconvex programming (under fixed period) into convex programming (under  $\hat{g}$ ).

We now can verify inequality (18) over  $x \in \mathcal{X}_0$  and  $u \in \mathcal{U}$ :

$$\theta \epsilon(x, u) \le \theta \left( \|Ax + Bu\| + \frac{d_v}{L_f} + d_w \right) \left( e^{L_f \hat{g}_{\text{max}}} - 1 \right) + d_w$$

$$\le 0.0498 \|x\| + 0.0188 \|u\| + 1.6476 \times 10^{-4}$$

$$= \rho \kappa(x, u) + d.$$

To define  $\mathcal{X}_{\mathcal{T}}$ , let us consider

$$\begin{split} V_f(\hat{f}(x+\tilde{x},h(x+\tilde{x}))) - V_f(x) \\ &= \|P(A_{\rm d} + BK)(x+\tilde{x})\| - \|Px\| \\ &\leq \|P(A_{\rm d} + BK)x\| - \|Px\| + \|P(A_{\rm d} + BK)\tilde{x}\| \\ &\leq -\kappa(x,Kx) + \|P(A_{\rm d} + BK)\tilde{x}\| \\ &\leq -0.08\|x\| - 0.1644\|x\| + \|P(A_{\rm d} + BK)\|d_{\tilde{x}} \end{split}$$

So the terminal set can be defined as

$$\mathcal{X}_{\mathcal{T}} = \{ x \in \mathbb{R}^n \mid ||Px|| \le 354.9257 \cdot d_{\tilde{x}} \}.$$

To ensure  $h(x) \in \mathcal{U}$  for all  $x \in \mathcal{X}_{\mathcal{T}} + \mathcal{B}\left((d_w + \epsilon_{\max})L_{\hat{f}}^{N-1}\right)$  where  $(d_w + \epsilon_{\max})L_{\hat{f}}^{N-1} = 0.0061$ , we check the bound on  $\|Kx\|$ :

$$|K(x+\tilde{x})| \le ||KP^L|| ||P(x+\tilde{x})||$$
  
 
$$\le 0.7944 \cdot (354.9257 \cdot d_{\tilde{x}} + 0.0061 ||P||) \le 2$$

where  $P^L = (P^\top P)^{-1} P^\top$  and  $\|\tilde{x}\| \le 0.0061$ . Solving this inequality , we can set  $d_{\tilde{x}} = 0.0069 \ge (d_w + \epsilon_{\max}) L_{\hat{f}}^{N-1}$ , which means that inequality (21) is satisfied.

To check the satisfaction of inequality (22), we first calculate  $\alpha_1^{-1} \left( \frac{d_w \theta + d}{1 - \rho} \right) = 0.0097$ . So

$$\max_{\|x\| \le 0.0097} [V(x) - (1 - \rho)\alpha_1(\|x\|)]$$
  
= 0.0751 < 0.0797 = d<sub>0</sub> - d<sub>w</sub>\theta - d.

We first set v(t)=w(t)=0. The top plot of Figure 2 shows the state trajectories that converge to the origin. The input also converges to zero, as shown in the middle plot. The bottom plot shows the history of the computation periods. It converges to 0.0167, which is consistent to the theoretical result  $\lim_{\|x\|\to 0} \hat{g}(x)=0.0167$  in this case. Figure 3 shows the history of  $V(\bar{x}(t_k))$ , which is monotonically decreasing to zero. Figure 4 shows the history of the actual state and the predicted state  $\hat{x}_k^1$ . Notice that  $\hat{x}_k^1$  is an approximation of  $x(t_{k+1})$  at  $t_k$ . We can find that the states are very close, though the approximation model is different from the actual plant.

In the second simulation, the disturbances and measure noises are added, where v(t) and w(t) are randomly chosen over  $[-d_v, d_v]$  and  $[-d_w, d_w]$ , respectively, with  $d_v = 0.1$  and  $d_w = 0.01$ . In the top plot of Figure 5 the state trajectories oscillate around the origin due to disturbances and noises. Accordingly, the inputs and the inter-sampling time intervals vary slightly, as shown in the middle and bottom plots. Meanwhile,  $V(x(t_k))$  also admits temporary increases in Figure (6).

### 5.2. Example 2

We consider a crane [38] with the horizontal trolley position  $x_1$ , the trolley velocity  $x_2$ , the excitation angle  $x_3$ , and the angular velocity of the mass point  $x_4$ . The control u is the acceleration of the trolley. Let  $x = (x_1, x_2, x_3, x_4)^{\top} \in \mathbb{R}^4$ . The crane model is described as follows:

$$\dot{x} = f(x, u) = \begin{pmatrix} x_2 \\ u \\ x_4 \\ -g\sin(x_3) - u\cos(x_3) - bx_4 \end{pmatrix}$$
 (28)

with the initial condition  $x_0 = (0.5, 0, \frac{2\pi}{3}, 0)^{\top}$ , where  $g = 9.81 m/s^2$ , b = 0.2 Js. The input constraint is assumed to be  $|u(t)| \le 1$ .

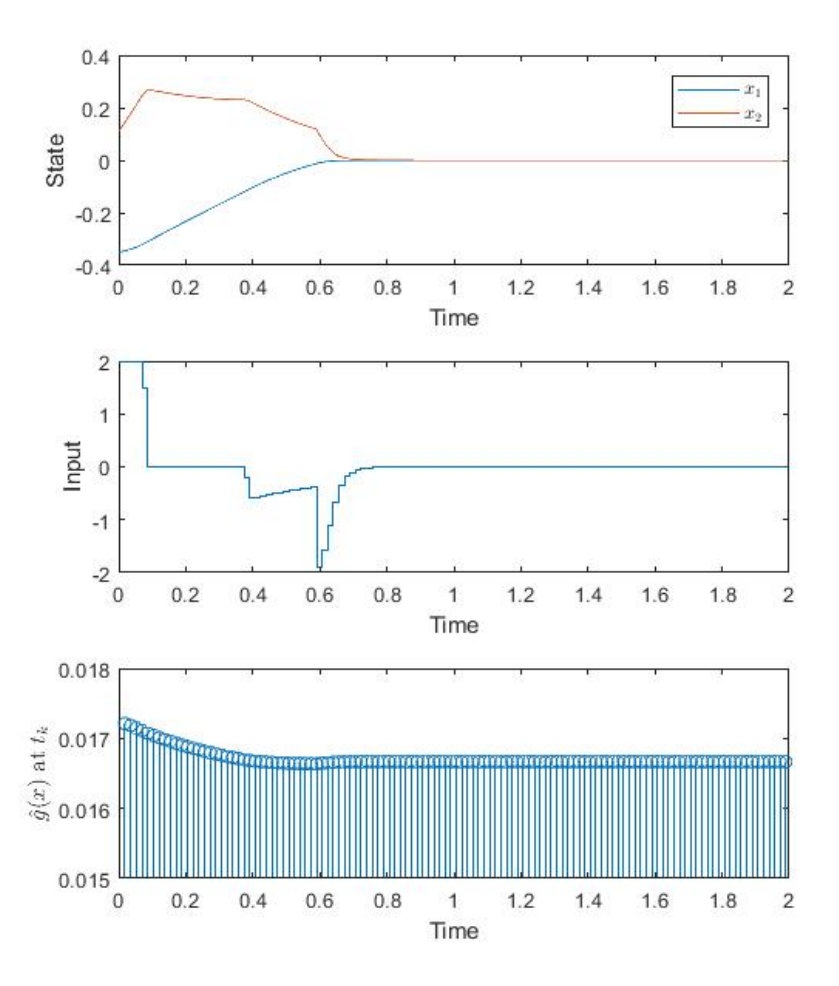


Figure 2. The state trajectories and computation periods with v(t)=w(t)=0. The top and middle plots show the convergence of the states and input, respectively. The bottom plot shows that the inter-sampling intervals that converge to  $\lim_{\|x\|\to 0} \hat{g}(x)=0.0167$ .

To formulate the MPC framework, we set the prediction horizon N=4. The cost function is

$$\kappa(x, u) = ||x|| + 0.15|u|, \quad V(x) = 2||x|| \tag{29}$$

The inter-sampling interval function  $\hat{g}(x, u)$  can be simply defined by

$$\hat{g}(x,u) = 0.01 (2 - \sin(x_3)). \tag{30}$$

The discrete-time model is then  $\hat{x}_k^{i+1}=\hat{x}_k^i+\hat{g}(\hat{x}_k,u_k^i)f(\hat{x}_k,u_k^i)$ . With this setting, we set  $d_x=8$ . Then we can numerically calculate  $L_f=9.8119,~L_u=1.4142,~L_{\hat{f}}=1.2277,~\theta=7.4358,~\epsilon_{\max}=0.1398,$  and  $d_{\tilde{x}}=0.2587.$  The approximation error is

$$\epsilon(x,u) = \hat{g}(x,u) \|f(x,u)\| \left(e^{L_f \hat{g}(x,u)} - 1\right).$$

We can see that  $\hat{g}_{\max} = \max_{x \in \mathcal{X}_0} \hat{g}(x, u) = 0.03 < T_{\max}(d_x) = 0.0321$ . We can verify (18) with d = 0 that

$$\theta \epsilon(x, u) \le 0.7491 ||x|| + 0.1080 |u| < \rho \kappa(x, u)$$

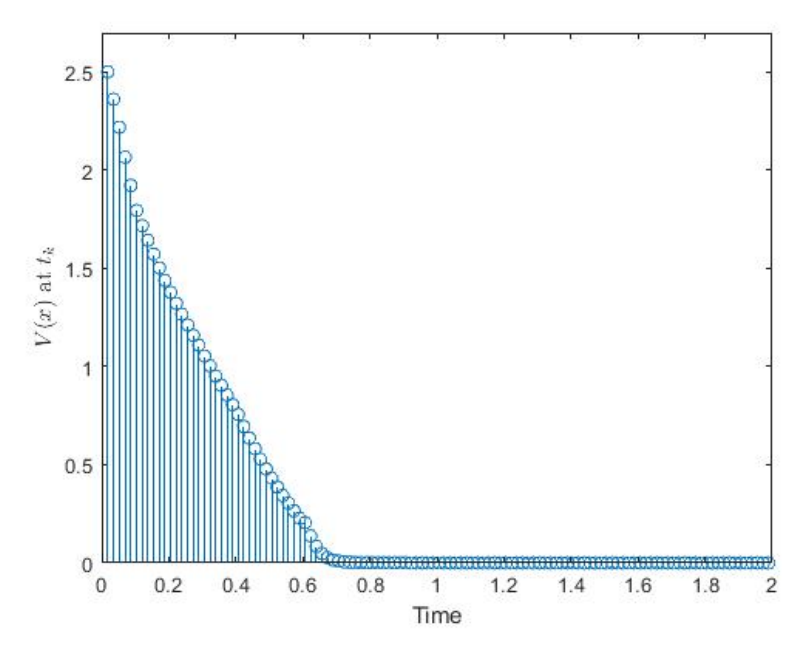


Figure 3. The history of  $V(\bar{x}(t_k))$  when v(t) = w(t) = 0, which monotonically decreases to zero.

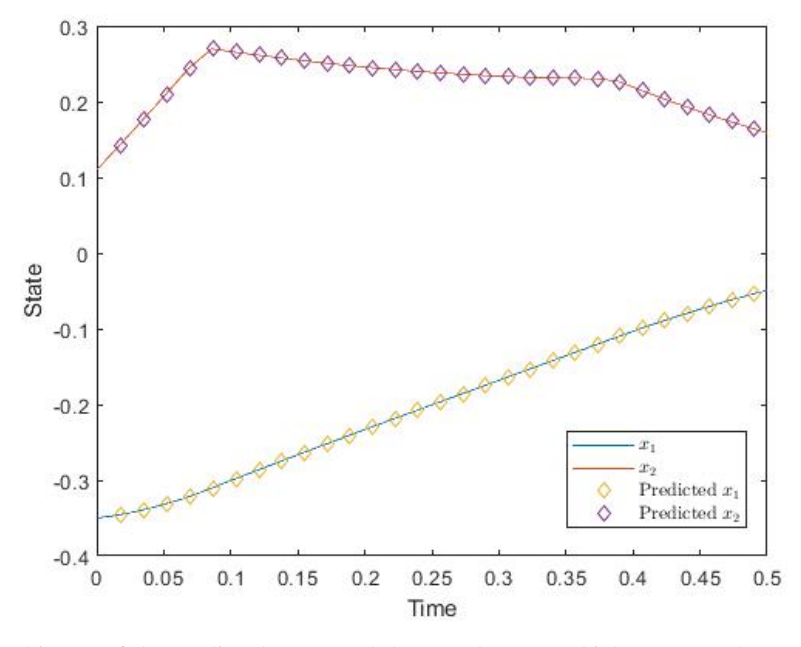


Figure 4. The history of the predicted states and the actual states, which are very close. It shows that the discrete-time model can approximate the plant at the sampling instants.

where  $\rho = 0.8$ . We leave  $\mathcal{X}_{\mathcal{T}} = \mathbb{R}^n$  since both the continuous-time and discrete-time systems can be stabilized by the control law  $h(x) = -0.1x_1 - 0.1x_2$ .

With this setting, we plot the state trajectories in Figure 7. We can find that the system asymptotically converge to the origin. Figure 8 shows that the inter-sampling time intervals vary dramatically during transience. Since  $\hat{g}$  is only related to  $x_3$  in this case, when  $x_3$  reaches the steady state, the time intervals also converges to a constant  $\lim_{x\to 0, u\to 0} \hat{g}(x,u) = 0.02$ . We then change the triggering function to  $\hat{g}(x,u) = 0.01(2 + \cos(x_3))$  with the other settings remaining the same. The

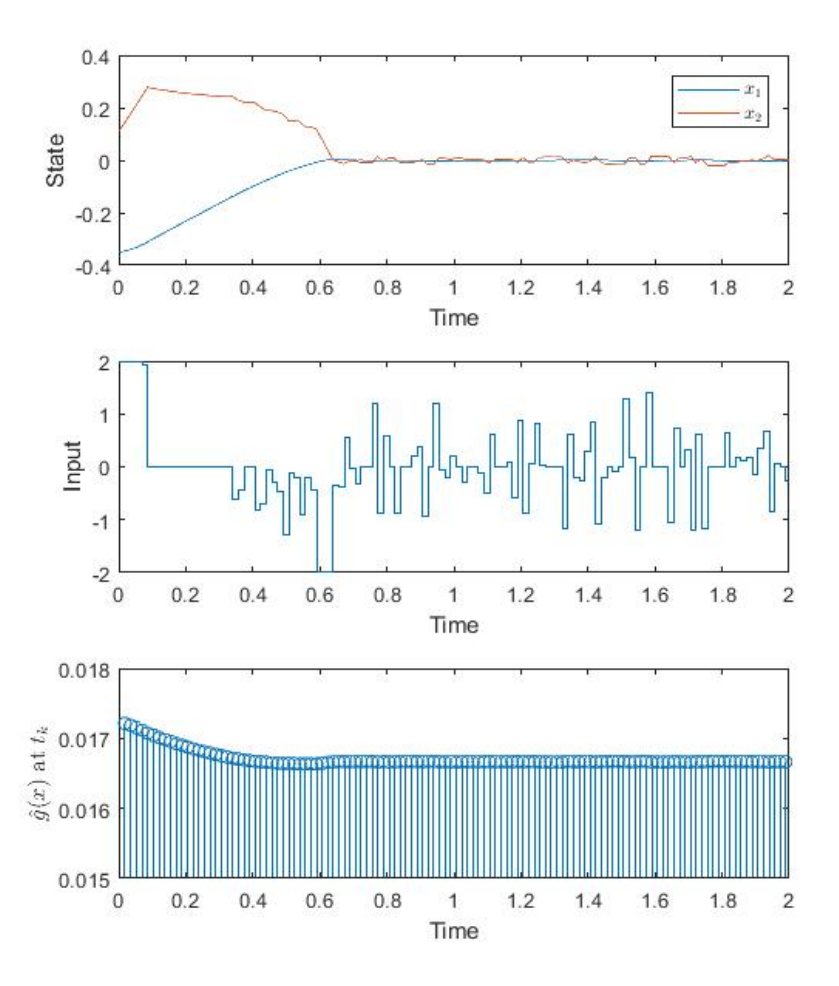


Figure 5. The state/input trajectories and computation periods in the presence of disturbances and noises. In the top plot, the states oscillate around the origin. Accordingly, the inputs and the inter-sampling time intervals vary slightly, as shown in the middle and bottom plots.

system is still stable, though the inter-sampling time intervals are completely different as shown in Figure 9. It demonstrates that our proposed principles can be applied to different triggering schemes.

# 6. CONCLUSIONS

This paper studies stability of nonlinear sampled-data systems controlled by discrete-time MPC, in the presence of exogenous disturbances and measurement noises. It suggests the co-design of the discrete-time FHOCP and the scheduling algorithms, where the scheduling scheme is coupled with the design of the discrete-time FHOCP in a sense that the model approximation error at the next sampling time instant must be bounded by a threshold function related to the running cost. Sufficient conditions are derived to guarantee uniform ultimate boundedness of the closed-loop system. The results are applicable to most conventional model approximation approaches and various scheduling schemes.

There are several many open problems in this framework. For instance, the choice of the scheduling function  $\hat{q}(x, u)$  is very flexible in this paper. On the other hand, however, it is not

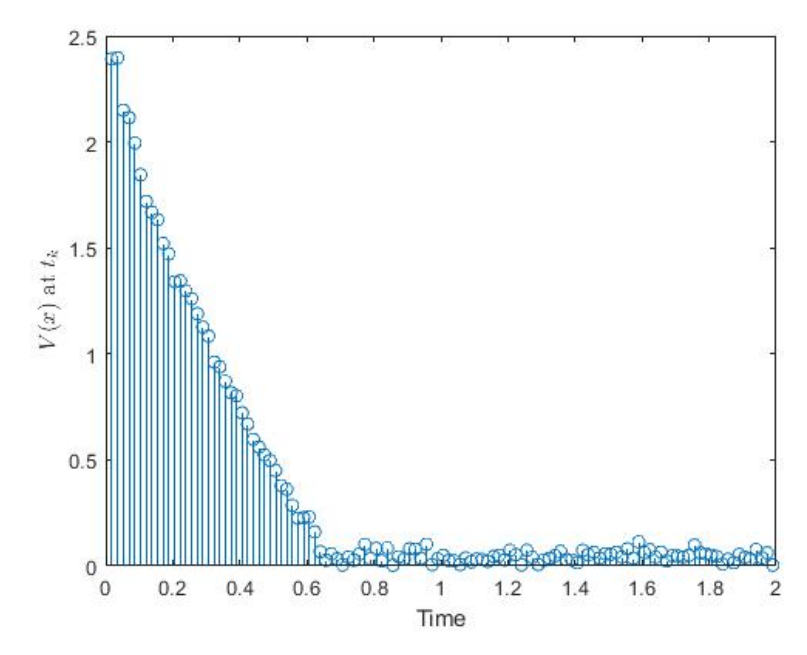


Figure 6. The history of  $V(\bar{x}(t_k))$  in the presence of disturbances and noises, where  $V(x(t_k))$  admits temporary increases.

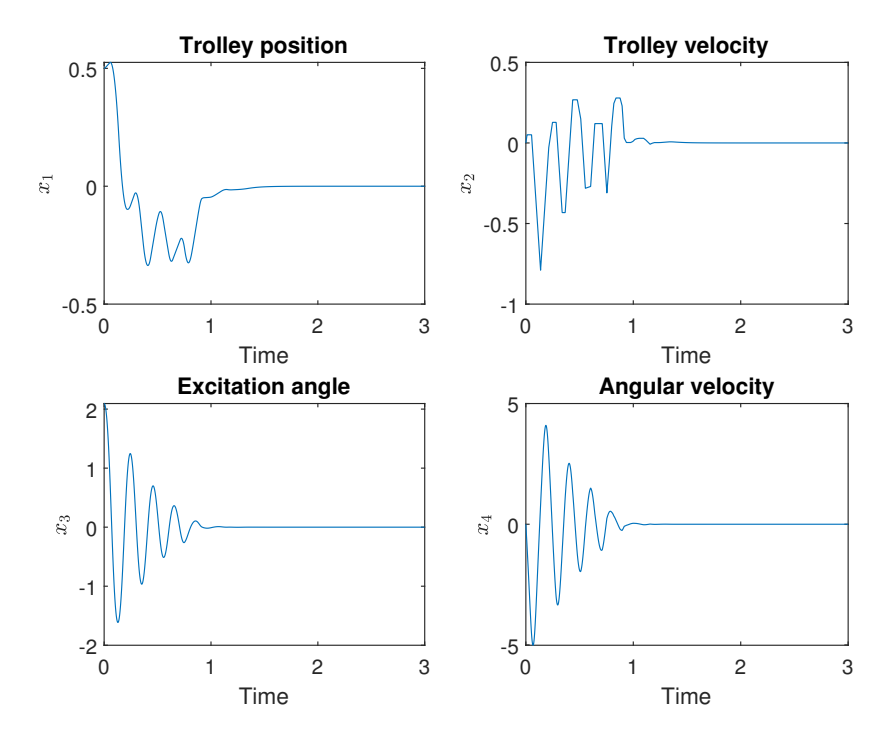


Figure 7. The state trajectories of the crane with  $\hat{g}(x, u) = 0.01 (2 - \sin(x_3))$ , which converge to the origin.

very clear that, for a specific system, which choice will be the best, with respect to computation load and the complexity of the resulting FHOCP. A more systematic approach to formulate the design procedure is expected, which will be studied in the future work. Tracking is another potential issue under this framework. When the reference signal is time-varying with high frequency, the

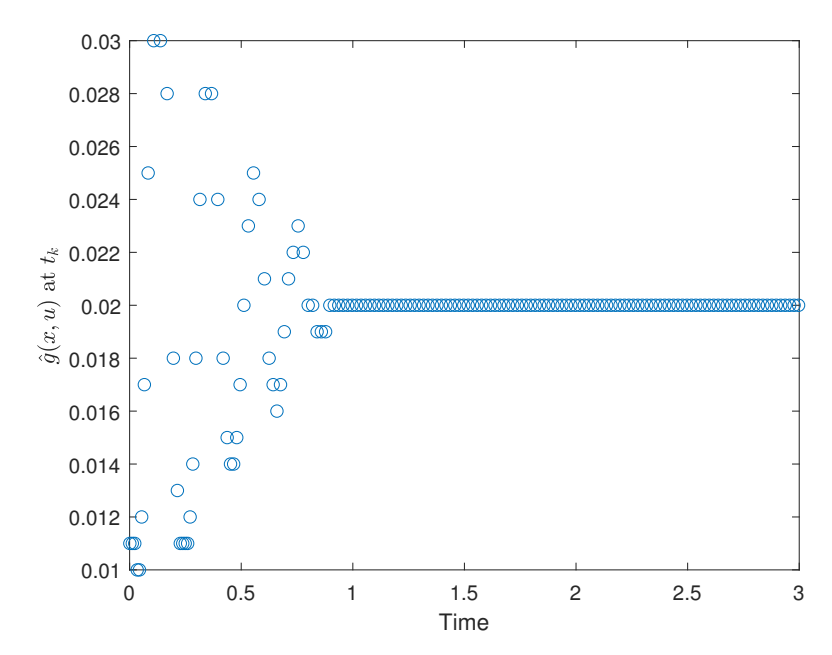


Figure 8. The history of the inter-sampling time intervals with  $\hat{g}(x,u) = 0.01 \ (2 - \sin(x_3))$ . The intersampling time intervals vary dramatically during transience and eventually converge to a constant, which is consistent to  $\lim_{x\to 0, u\to 0} \hat{g}(x,u) = 0.02$ .

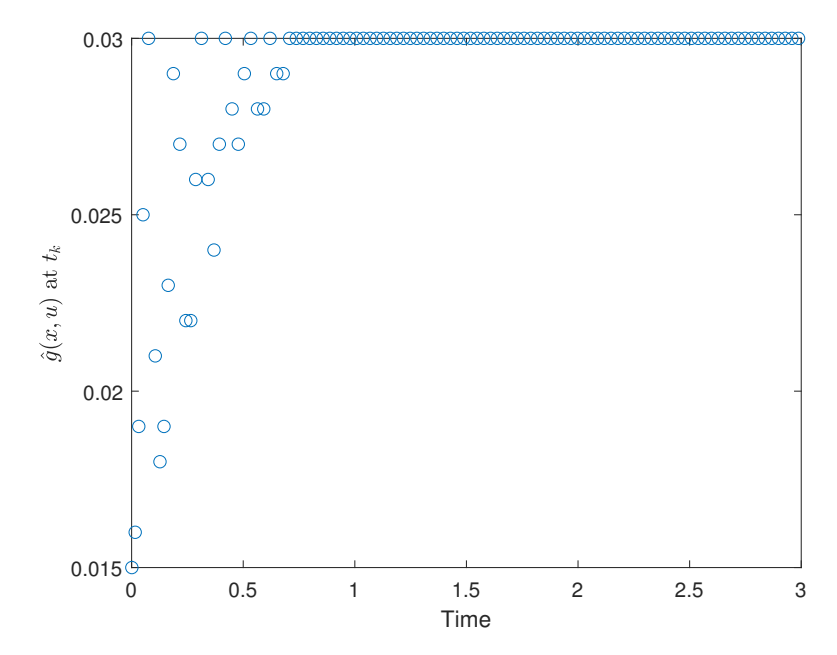


Figure 9. The history of the inter-sampling time intervals with  $\hat{g}(x,u) = 0.01(2 + \cos(x_3))$ . The intersampling time intervals are completely different from the case when  $\hat{g}(x,u) = 0.01(2 - \sin(x_3))$ .

approximation model may have to be accurate enough to capture variations in the reference signal; otherwise, undersampling may occur. How to balance the relation between the approximation model, the scheduling scheme, and the reference signals in this framework will be investigated in the future.

### A. APPENDIX: PROOF OF THEOREM 3.1

First of all, we construct a sequence of control inputs for the prediction model in (3) at the (k+1)th computation cycle with the initial condition  $\hat{x}_{k+1}^0 = \bar{x}(t_{k+1})$ :

$$\hat{u}_{k+1}^{i} = \begin{cases} \hat{u}_{k}^{i+1,*}, & i = 0, 1, ..., N-2\\ \text{To Be Determined. } i = N-1 \end{cases}$$
 (31)

With  $\hat{u}_{k+1}^i$  and  $\hat{x}_{k+1}^0 = \bar{x}(t_{k+1})$ , the discrete-time model in (3a) will generate the predicted states at the (k+1)th computation cycle as  $\hat{x}_{k+1}^i$  for  $i=1,2,\cdots,N-1$ . Notice that  $\hat{x}_{k+1}^N$  is undefined yet because  $\hat{u}_{k+1}^{N-1}$  is not specified yet.

Then we introduce three lemmas (Lemma A.1–A.3).

#### Lemma A.1

Suppose that Assumption 3.2 holds. If  $\bar{x}(t_k) \in \mathcal{V}_0$  and

$$t_{k+1} - t_k \le T_{\max}(d_x) \tag{32}$$

hold, where  $T_{\max}(d_x)$  is defined in (23), then  $x(t) \in \mathcal{B}(d_x)$  for  $t \in [t_k, t_{k+1}]$ .

# Proof

We prove the statement by contradiction. Suppose that  $x(t) \notin \mathcal{B}(d_x)$  for some  $t \in [t_k, t_{k+1}]$ . Because  $\bar{x}(t_k) \in \mathcal{V}_0$ , we know  $V(\bar{x}(t_k)) \leq d_0$ . By Assumption 3.2,

$$\alpha_1(\|\bar{x}(t_k)\|) \le \kappa(\bar{x}(t_k), \hat{u}_k^{0,*}) \le V(\bar{x}(t_k)) \le d_0$$

holds. So  $\|\bar{x}(t_k)\| \le \alpha_1^{-1}(d_0)$  and therefore  $x(t_k) \in \mathcal{B}\left(\alpha_1^{-1}(d_0) + d_w\right) \subseteq \mathcal{B}(d_x)$ , i.e.,  $\|x(t_k)\| < d_x$ . Since x(t) is continuous, there must exist  $t^* \in (t_k, t_{k+1})$  such that

$$||x(t^*)|| = d_x, (33)$$

$$||x(t)|| < d_x, \quad \forall t \in [t_k, t^*).$$
 (34)

Consider the system in (1) over  $[t_k, t^*]$ . By inequality (34), we know  $x(t) \in \mathcal{B}(d_x)$  for any  $t \in [t_k, t^*]$ . With  $u(t) = u(t_k) \in \mathcal{U}$ ,

$$\frac{d}{dt}||x(t)|| \le ||f(x(t), u(t_k))|| + ||v(t)||$$

$$\le L_f||x(t)|| + L_u||u(t_k)|| + d_v.$$

Solving this inequality yields

$$||x(t)|| \le ||x(t_k)|| e^{L_f(t-t_k)} + \frac{L_u ||u(t_k)|| + d_v}{L_f} \left( e^{L_f(t-t_k)} - 1 \right)$$

$$< (||\bar{x}(t_k)|| + d_w) e^{L_f(t_{k+1}-t_k)}$$

$$+ \frac{L_u ||u(t_k)|| + d_v}{L_f} \left( e^{L_f(t_{k+1}-t_k)} - 1 \right)$$

$$\le (\alpha_1^{-1}(d_0) + d_w) e^{L_f T_{\max}(d_x)}$$

$$+ \frac{L_u \max_{u \in \mathcal{U}} ||u|| + d_v}{L_f} \left( e^{L_f T_{\max}(d_x)} - 1 \right) = d_x.$$

for any  $t \in [t_k, t^*]$ , where the last equivalence comes from the definition of  $T_{\max}(d_x)$  in (23). The inequality above is contradicted with  $||x(t^*)|| = d_x$ . Therefore, the proof is completed.

The following lemma quantifies the error between the predicted states computed at the kth and k+1th computation cycles.

Lemma A.2

If  $\bar{x}(t_k) \in \mathcal{V}_0$ ,  $\bar{x}(t_{k+1}) \in \mathcal{B}(d_x + d_w)$ , and Assumption 3.2–3.3 hold, then

$$\|\hat{x}_{k+1}^{i-1} - \hat{x}_{k}^{i,*}\| \le (d_w + \epsilon_k) L_{\hat{f}}^{i-1}, \ i = 1, 2, ..., N.$$
(35)

holds where

$$\epsilon_k = \epsilon \left( \bar{x}(t_k), \hat{u}_k^{0,*} \right). \tag{36}$$

Proof

We prove the statement using mathematical induction. By the assumption  $\bar{x}(t_k) \in \mathcal{V}_0 \subseteq \mathcal{B}\left(\alpha_1^{-1}(d_0)\right)$ , we know that  $x(t_k) \in \mathcal{B}(d_x)$  by equation (2). Since x(t) is the solution to the system in (1) with  $u(t) = \hat{u}_k^{0,*}$  over  $[t_k, t_{k+1}]$  starting from  $x(t_k)$ , by inequality (14),

$$\left\| x \left( t_k + \hat{g}(\bar{x}(t_k), \hat{u}_k^{0,*}) \right) - \hat{f}\left(\bar{x}(t_k), \hat{u}_k^{0,*}\right) \right\|$$

$$\leq \epsilon \left( \bar{x}(t_k), \hat{u}_k^{0,*} \right) = \epsilon_k.$$

By equation (5), we know  $t_{k+1} = t_k + \hat{g}(\bar{x}(t_k), \hat{u}_k^{0,*})$  and by equation (3a), we have  $\hat{x}_k^{1,*} = \hat{f}(\bar{x}(t_k), \hat{u}_k^{0,*})$ . So the inequality above implies

$$\left\| x\left(t_{k+1}\right) - \hat{x}_{k}^{1,*} \right\| \le \epsilon_{k}. \tag{37}$$

So for i = 1 we have

$$\|\hat{x}_{k+1}^{0} - \hat{x}_{k}^{1,*}\| = \|\bar{x}(t_{k+1}) - \hat{x}_{k}^{1,*}\|$$

$$= \|\bar{x}(t_{k+1}) - x(t_{k+1}) + x(t_{k+1}) - \hat{x}_{k}^{1,*}\|$$

$$\leq \|\bar{x}(t_{k+1}) - x(t_{k+1})\| + \|x(t_{k+1}) - \hat{x}_{k}^{1,*}\|$$

$$\leq d_{w} + \epsilon_{k}.$$

Next we assume that inequality (35) holds for i = p - 1, i.e.,

$$\|\hat{x}_{k+1}^{p-2} - \hat{x}_k^{p-1,*}\| \le (d_w + \epsilon_k) L_{\hat{f}}^{p-2}$$
(38)

and prove that inequality (35) also holds for i = p.

According to equation (3a) and the definition of  $\hat{u}_{k+1}^i$  in equation (31), we have

$$\hat{x}_k^{p,*} = \hat{f}(\hat{x}_k^{p-1,*}, \hat{u}_k^{p-1,*}) \quad \text{and}$$

$$\hat{x}_{k+1}^{p-1} = \hat{f}(\hat{x}_{k+1}^{p-2}, \hat{u}_{k+1}^{p-2}) = \hat{f}(\hat{x}_{k+1}^{p-2}, \hat{u}_k^{p-1,*}).$$

Therefore,

$$\begin{split} &\|\hat{x}_{k+1}^{p-1} - \hat{x}_k^{p,*}\| \\ = &\|\hat{f}(\hat{x}_{k+1}^{p-2}, \hat{u}_k^{p-1,*}) - \hat{f}(\hat{x}_k^{p-1,*}, \hat{u}_k^{p-1,*})\|. \end{split}$$

Since  $\bar{x}(t_k) \in \mathcal{B}\left(\alpha_1^{-1}(d_0)\right) \subset \mathcal{B}(d_x + d_w)$  and  $\bar{x}(t_{k+1}) \in \mathcal{B}(d_x + d_w)$ , we have  $\hat{x}_{k+1}^{p-2}$ ,  $\hat{x}_k^{p-1,*} \in \mathcal{X}_{\hat{f}}$  for any  $p \leq N$ . With  $\hat{u}_k^{p-1,*} \in \mathcal{U}$ , by inequality (10) in Assumption 3.3 and inequality (38), we have

$$\|\hat{x}_{k+1}^{p-1} - \hat{x}_{k}^{p,*}\| \le L_{\hat{f}} \|\hat{x}_{k+1}^{p-2} - \hat{x}_{k}^{p-1,*}\|$$

$$\le (d_{w} + \epsilon_{k}) L_{\hat{f}}^{p-1},$$

which completes the proof.

### Lemma A.3

Suppose that Assumption 3.2-3.5 hold and

$$\bar{x}(t_k) \in \mathcal{V}_0, \ \bar{x}(t_{k+1}) \in \mathcal{B}(d_x + d_w).$$

If inequality (21) holds and there exists an admissible optimal solution  $\left\{\hat{x}_k^{i,*}, \hat{u}_k^{i,*}\right\}_{i=0}^{N-1}$  to the FHOCP in (4) at the kth computation cycle, then  $\left\{\hat{x}_{k+1}^i\right\}_{i=0}^N$  and  $\left\{\hat{u}_{k+1}^i\right\}_{i=0}^{N-1}$  are admissible to the FHOCP at the k+1th computation cycle, where  $\hat{u}_{k+1}^i$  is defined in (31) for  $i=0,1,\cdots,N-2$ 

$$\hat{u}_{k+1}^{N-1} = h(\hat{x}_{k+1}^{N-1}). \tag{39}$$

Moreover, the following inequality

$$V(\bar{x}(t_{k+1})) - V(\bar{x}(t_k)) \le d_w \theta + d - (1 - \rho) \alpha_1(\|\bar{x}(t_k)\|)$$
(40)

holds.

### Proof

We first show that  $\hat{u}_{k+1}^{N-1} \in \mathcal{U}$  and the state trajectory  $\left\{\hat{x}_{k+1}^i\right\}_{i=0}^N$ , generated by the control sequence  $\left\{\hat{u}_{k+1}^i\right\}_{i=0}^{N-1}$ , is admissible to the FHOCP. Since the assumptions in Lemma A.2 hold, equation (35) holds, which, together with

inequality (21), implies

$$\|\hat{x}_{k+1}^{N-1} - \hat{x}_k^{N,*}\| \le (d_w + \epsilon_k) L_{\hat{f}}^{N-1} \le d_{\tilde{x}}. \tag{41}$$

So there exists  $\tilde{x} \in \mathcal{B}(d_{\tilde{x}})$  such that

$$\hat{x}_{k+1}^{N-1} = \hat{x}_k^{N,*} + \tilde{x}. \tag{42}$$

Notice that

$$\hat{x}_{k+1}^{N} = \hat{f}\left(\hat{x}_{k+1}^{N-1}, \hat{u}_{k+1}^{N-1}\right) = \hat{f}\left(\hat{x}_{k+1}^{N-1}, h\left(\hat{x}_{k+1}^{N-1}\right)\right) 
= \hat{f}\left(\hat{x}_{k}^{N,*} + \tilde{x}, h\left(\hat{x}_{k}^{N,*} + \tilde{x}\right)\right).$$
(43)

Because  $\left\{\hat{x}_k^{i,*}, \hat{u}_k^{i,*}\right\}_{i=0}^{N-1}$  is admissible at the kth computation cycle,  $\hat{x}_k^{N,*} \in \mathcal{X}_{\mathcal{T}}$  holds and therefore  $\hat{x}_{k+1}^{N-1} \in \mathcal{X}_{\mathcal{T}} + \mathcal{B}\left((d_w + \epsilon_{\max})L_{\hat{f}}^{N-1}\right). \text{ So by equation (16) in Assumption 3.4, } \hat{u}_{k+1}^{N-1} = h(\hat{x}_{k+1}^{N-1}) \in \mathcal{U} \text{ holds. Meantime, because } \mathcal{X}_{\mathcal{T}} \text{ is robust positively invariant with respect to the system in (43), } \hat{x}_{k+1}^{N} \in \mathcal{X}_{\mathcal{T}} \text{ holds. So } \left\{\hat{x}_{k+1}^{i}\right\}_{i=0}^{N} \text{ with } \left\{\hat{u}_{k+1}^{i}\right\}_{i=0}^{N-1} \text{ is admissible to the FHOCP at the } k+1\text{th computation cycle.}$  Let  $J[\hat{\mathbf{u}}_{k+1}|\bar{x}(t_{k+1})]$  be the cost of the FHOCP generated by  $\hat{\mathbf{u}}_{k+1} = \left\{\hat{u}_{k+1}^i\right\}_{i=0}^{N-1}$  with the initial condition  $\bar{x}(t_{k+1})$ . Consider

$$J[\hat{\mathbf{u}}_{k+1}|\bar{x}(t_{k+1})] - V(\bar{x}(t_{k}))$$

$$= \sum_{i=0}^{N-1} \kappa \left(\hat{x}_{k+1}^{i}, \hat{u}_{k+1}^{i}\right) + V_{f}\left(\hat{x}_{k+1}^{N}\right) - V(\bar{x}(t_{k}))$$

$$= \sum_{i=0}^{N-2} \kappa \left(\hat{x}_{k+1}^{i}, \hat{u}_{k+1}^{i}\right) + \kappa \left(\hat{x}_{k+1}^{N-1}, \hat{u}_{k+1}^{N-1}\right) + V_{f}\left(\hat{x}_{k+1}^{N}\right)$$

$$- V(\bar{x}(t_{k})) + V_{f}\left(\hat{x}_{k+1}^{N-1}\right) - V_{f}\left(\hat{x}_{k+1}^{N-1}\right)$$

$$+ \kappa \left(\hat{x}_{k}^{0,*}, \hat{u}_{k}^{0,*}\right) - \kappa \left(\hat{x}_{k}^{0,*}, \hat{u}_{k}^{0,*}\right)$$

$$= \underbrace{\kappa \left(\hat{x}_{k+1}^{N-1}, \hat{u}_{k+1}^{N-1}\right) + V_{f}(\hat{x}_{k+1}^{N}) - V_{f}(\hat{x}_{k+1}^{N-1})}_{\Psi}$$

$$- \kappa \left(\hat{x}_{k}^{0,*}, \hat{u}_{k}^{0,*}\right) + \Phi$$

$$(44)$$

where

$$\Phi = \sum_{i=0}^{N-2} \kappa \left( \hat{x}_{k+1}^i, \hat{u}_{k+1}^i \right) + V_f \left( \hat{x}_{k+1}^{N-1} \right) + \kappa \left( \hat{x}_k^{0,*}, \hat{u}_k^{0,*} \right) - V(\bar{x}(t_k)).$$

Given  $\hat{x}_{k+1}^{N-1} \in \mathcal{X}_{\mathcal{T}} + \mathcal{B}\left((d_w + \epsilon_{\max})L_{\hat{f}}^{N-1}\right)$  and inequality (17) in Assumption 3.4, we have  $\Psi \leq 0$ , since  $\hat{x}_{k+1}^N = \hat{f}\left(\hat{x}_{k+1}^{N-1}, h(\hat{x}_{k+1}^{N-1})\right)$ . Therefore, equation (44) implies

$$J[\hat{\mathbf{u}}_{k+1}|\bar{x}(t_{k+1})] - V(\bar{x}(t_k)) \le \Phi - \kappa \left(\hat{x}_k^{0,*}, \hat{u}_k^{0,*}\right). \tag{45}$$

Consider  $\Phi$ . Notice that the first term in  $\Phi$  can be written as

$$\sum_{i=0}^{N-2} \kappa\left(\hat{x}_{k+1}^i, \hat{u}_{k+1}^i\right) = \sum_{i=1}^{N-1} \kappa\left(\hat{x}_{k+1}^{i-1}, \hat{u}_{k+1}^{i-1}\right)$$

According to equation (4),

$$V(\bar{x}(t_k)) = \sum_{i=0}^{N-1} \kappa \left( \hat{x}_k^{i,*}, \hat{u}_k^{i,*} \right) + V_f \left( \hat{x}_k^{N,*} \right).$$

Therefore, using this equation to replace  $V(\bar{x}(t_k))$  in  $\Phi$ ,

$$\Phi = \sum_{i=1}^{N-1} \kappa \left( \hat{x}_{k+1}^{i-1}, \hat{u}_{k+1}^{i-1} \right) + V_f \left( \hat{x}_{k+1}^{N-1} \right) - \sum_{i=1}^{N-1} \kappa \left( \hat{x}_k^{i,*}, \hat{u}_k^{i,*} \right) - V_f \left( \hat{x}_k^{N,*} \right).$$
(46)

By equation (31),  $\hat{u}_{k+1}^{i-1} = \hat{u}_k^{i,*}$  for  $i = 1, 2, \dots, N-1$ . So

$$\Phi \leq \sum_{i=1}^{N-1} \left| \kappa \left( \hat{x}_{k+1}^{i-1}, \hat{u}_{k+1}^{i-1} \right) - \kappa \left( \hat{x}_{k}^{i,*}, \hat{u}_{k}^{i,*} \right) \right| 
+ \left| V_{f} \left( \hat{x}_{k+1}^{N-1} \right) - V_{f} \left( \hat{x}_{k}^{N,*} \right) \right| 
\leq \sum_{i=1}^{N-1} L_{\kappa} \left\| \hat{x}_{k+1}^{i-1} - \hat{x}_{k}^{i,*} \right\| + L_{V_{f}} \left\| \hat{x}_{k+1}^{N-1} - \hat{x}_{k}^{N,*} \right\|,$$

where the last inequality comes from equation (11) and (12) in Assumption 3.3, given  $\bar{x}(t_k), \ \bar{x}(t_{k+1}) \in \mathcal{B}(d_x + d_w)$  and therefore  $\hat{x}_{k+1}^{i-1}, \hat{x}_k^{i,*} \in \mathcal{X}_{\hat{f}}$  for  $i = 1, 2 \cdots, N$ .

By Lemma A.2, 
$$\|\hat{x}_{k+1}^{i-1} - \hat{x}_{k}^{i,*}\| \leq (d_w + \epsilon_k) L_{\hat{f}}^{i-1}$$
 for  $i = 1, 2, \dots, N$ . Therefore,

$$\Phi \le (d_w + \epsilon_k) \underbrace{\left( \sum_{i=1}^{N-1} L_{\kappa} L_{\hat{f}}^{i-1} + L_{V_f} L_{\hat{f}}^{N-1} \right)}_{\theta}.$$

With the inequality above and inequality (18) in Assumption 3.5, inequality (45) can be further simplified as

$$J[\hat{\mathbf{u}}_{k+1}|\bar{x}(t_{k+1})] - V(\bar{x}(t_k))$$

$$\leq -\kappa \left(\hat{x}_k^{0,*}, \hat{u}_k^{0,*}\right) + (d_w + \epsilon_k)\theta$$

$$\leq -(1 - \rho) \kappa \left(\hat{x}_k^{0,*}, \hat{u}_k^{0,*}\right) + d_w\theta + d.$$

Therefore,

$$V(\bar{x}(t_{k+1})) - V(\bar{x}(t_k))$$

$$= \min_{\hat{\mathbf{u}}_{k+1}} J[\hat{\mathbf{u}}_{k+1} | \bar{x}(t_{k+1})] - V(\bar{x}(t_k))$$

$$\leq -(1 - \rho) \kappa \left(\hat{x}_k^{0,*}, \hat{u}_k^{0,*}\right) + d_w \theta + d$$

$$\leq -(1 - \rho) \alpha_1 (\|\bar{x}(t_k)\|) + d_w \theta + d,$$

where the last inequality comes from Assumption 3.2 and the fact  $\hat{x}_k^{0,*} = \bar{x}(t_k)$ .

Now we are ready to prove Theorem 3.1. It will be shown that

The FHOCP is feasible at 
$$t_{k+1}$$
, (47)

$$\bar{x}(t_{k+1}) \in \mathcal{V}_0, \quad \text{and}$$

$$V(\bar{x}(t_{k+1})) - V(\bar{x}(t_k)) \le d_w \theta + d - (1 - \rho) \alpha_1(\|\bar{x}(t_k)\|)$$
(49)

hold for  $k = 0, 1, 2, \dots$ , using mathematical induction.

For k=0,  $\bar{x}(t_0)\in\mathcal{V}_0$  by the assumption. Since the hypotheses of Lemma A.1 hold for k=0, we have  $x(t_1)\in\mathcal{B}(d_x)$  and therefore  $\bar{x}(t_1)\in\mathcal{B}(d_x+d_w)$ . Meanwhile, with  $\bar{x}(t_0)\in\mathcal{V}_0$  and the fact that the FHOCP in (4) admits a feasible solution at  $t_0$ , the hypotheses of Lemma A.3 are satisfied for k=0, which implies that  $\left\{\hat{x}_1^i\right\}_{i=0}^N$  and  $\left\{\hat{u}_1^i\right\}_{i=0}^{N-1}$  are admissible to the FHOCP at  $t_1$  with the initial condition  $\bar{x}(t_1)$ , and

$$V(\bar{x}(t_1)) - V(\bar{x}(t_0)) \le -(1 - \rho) \alpha_1 (\|\bar{x}(t_0)\|) + d_w \theta + d.$$
(50)

There are two cases to be discussed. If  $\|\bar{x}(t_0)\| \geq \alpha_1^{-1}\left(\frac{d_w\theta+d}{1-\rho}\right)$ , then  $V(\bar{x}(t_1)) \leq V(\bar{x}(t_0)) \leq d_0$  and therefore  $\bar{x}(t_1) \in \mathcal{V}_0$ . If  $\|\bar{x}(t_0)\| < \alpha_1^{-1}\left(\frac{d_w\theta+d}{1-\rho}\right)$ , then with  $V(\bar{x}(t_0)) \leq \alpha_2(\|\bar{x}(t_0)\|)$ , we have

$$V(\bar{x}(t_1)) \le \alpha_2(\|\bar{x}(t_0)\|) - (1 - \rho) \alpha_1(\|\bar{x}(t_0)\|) + d_w\theta + d.$$

By inequality (22), we know  $V(\bar{x}(t_1)) \leq d_0$ . Therefore,  $\bar{x}(t_1) \in \mathcal{V}_0$  holds in either case.

Assume that the statements in (47) – (49) hold for k = p - 1. We will show that they will also hold for k = p.

By Lemma A.1, inequality (20), together with  $\bar{x}(t_p) \in \mathcal{V}_0$ , implies  $x(t_{p+1}) \in \mathcal{B}(d_x)$  and therefore  $\bar{x}(t_{p+1}) \in \mathcal{B}(d_x + d_w)$ . Since the hypotheses of Lemma A.3 hold for k = p, we know that the

FHOCP is feasible at  $t_{p+1}$  and

$$V(\bar{x}(t_{p+1})) - V(\bar{x}(t_p)) \le d_w \theta + d - (1 - \rho) \alpha_1(\|\bar{x}(t_p)\|).$$

Following the previous analysis, two cases can be discussed. If  $\|\bar{x}(t_p)\| \ge \alpha_1^{-1} \left(\frac{d_w\theta+d}{1-\rho}\right)$ , then  $V(\bar{x}(t_{p+1})) \le V(\bar{x}(t_p)) \le d_0$ . If  $\|\bar{x}(t_p)\| < \alpha_1^{-1} \left(\frac{d_w\theta+d}{1-\rho}\right)$ , then with  $V(\bar{x}(t_p)) \le \alpha_2(\|\bar{x}(t_p)\|)$  by Assumption 3.2,

$$V(\bar{x}(t_{p+1})) \le \alpha_2(\|\bar{x}(t_p)\|) - (1 - \rho) \alpha_1(\|\bar{x}(t_p)\|) + d_m\theta + d.$$

By inequality (22), we know  $V(\bar{x}(t_{p+1})) \leq d_0$ . Overall,  $\bar{x}(t_{p+1}) \in \mathcal{V}_0$  holds for both cases. So the statements in (47) – (49) hold for all  $k \in \mathbb{Z}_0^+$ .

Since  $\bar{x}(t_k) \in \mathcal{V}_0$  for all  $k \in \mathbb{Z}_0^+$ , we know by Assumption 3.2 that  $\alpha_1(\|\bar{x}(t_k)\|) \leq V(\bar{x}(t_k)) \leq \alpha_2(\|\bar{x}(t_k)\|)$ , which, together with inequality (49), implies that  $\{\bar{x}(t_k)\}_{k=0}^{\infty}$  is uniformly ultimately bounded. For any  $t \in [t_k, t_{k+1})$ , we solve the following differential inequality

$$\frac{d}{dt}||x(t) - \bar{x}(t_k)|| \le ||f(x(t), \hat{u}_k^{0,*})|| + ||v(t)|| \le f_{\max} + d_v,$$

where  $f_{\max} = \max_{x \in \mathcal{B}(d_x), u \in \mathcal{U}} \|f(x, u)\|$ , with the initial condition  $\|x(t_k) - \bar{x}(t_k)\| \le d_w$ . It implies that for any  $t \in [t_k, t_{k+1})$ 

$$||x(t) - \bar{x}(t_k)|| \le d_w + (f_{\max} + d_v) \, \hat{g}(\bar{x}(t_k), \hat{u}_k^{0,*})$$
  
$$\le d_w + (f_{\max} + d_v) \max_{\bar{x} \in \mathcal{V}_0, \ u \in \mathcal{U}} \hat{g}(\bar{x}, u).$$

So x(t) is also uniformly ultimately bounded.

### ACKNOWLEDGEMENT

The authors gratefully acknowledge the partial financial support of the National Science Foundation.

#### REFERENCES

- Mayne DQ, Rawlings JB, Rao CV, Scokaert PO. Survey constrained model predictive control: Stability and optimality. Automatica (Journal of IFAC) 2000; 36(6):789–814.
- 2. Morari M, Lee JH. Model predictive control: past, present and future. *Computers & Chemical Engineering* 1999; 23(4-5):667–682.
- Fontes FA. A general framework to design stabilizing nonlinear model predictive controllers. Systems & Control Letters 2001; 42(2):127–143.
- Hu LS, Huang B, Cao YY. Robust digital model predictive control for linear uncertain systems with saturations. IEEE Transactions on Automatic Control 2004; 49(5):792–796.
- Magni L, Scattolini R. Model predictive control of continuous-time nonlinear systems with piecewise constant control. *IEEE Transactions on Automatic Control* 2004; 49(6):900–906.
- Rubagotti M, Raimondo DM, Ferrara A, Magni L. Robust model predictive control with integral sliding mode in continuous-time sampled-data nonlinear systems. *IEEE Transactions on Automatic Control* 2011; 56(3):556–570.
- Grüne L, Nesic D. Optimization-based stabilization of sampled-data nonlinear systems via their approximate discrete-time models. SIAM Journal on Control and Optimization 2003; 42(1):98–122.
- 8. Nešić D, Grüne L. A receding horizon control approach to sampled-data implementation of continuous-time controllers. *Systems & Control Letters* 2006; **55**(8):660–672.
- Gyurkovics É, Elaiw AM. Conditions for MPC based stabilization of sampled-data nonlinear systems via discretetime approximations. Assessment and Future Directions of Nonlinear Model Predictive Control. Springer, 2007; 35–48.
- Sopasakis P, Patrinos P, Sarimveis H. MPC for sampled-data linear systems: Guaranteeing constraint satisfaction in continuous-time. *IEEE Transactions on Automatic Control* 2014; 59(4):1088–1093.
- Farina M, Scattolini R. Tube-based robust sampled-data MPC for linear continuous-time systems. Automatica 2012; 48(7):1473–1476.

- 12. Brunner FD, Heemels W, Allgöwer F. Robust event-triggered MPC for constrained linear discrete-time systems with guaranteed average sampling rate. *IFAC-PapersOnLine* 2015; **48**(23):117–122.
- Eqtami A, Dimarogonas DV, Kyriakopoulos KJ. Event-triggered control for discrete-time systems. Proceedings of American Control Conference, IEEE, 2010; 4719

  –4724.
- 14. Eqtami A, Dimarogonas DV, Kyriakopoulos KJ. Event-triggered strategies for decentralized model predictive controllers. *Proceedings of the 18th IFAC World Congress* 2011; **44**(1):10 068–10 073.
- Eqtami A, Dimarogonas DV, Kyriakopoulos KJ. Novel event-triggered strategies for model predictive controllers. Proceedings of the 50th IEEE Conference on Decision and Control and European Control Conference, IEEE, 2011; 3392–3397.
- Ferrara A, Incremona GP, Magni L. Model-based event-triggered robust MPC/ISM. Proceedings of European Control Conference, IEEE, 2014; 2931–2936.
- 17. Lehmann D, Henriksson E, Johansson KH. Event-triggered model predictive control of discrete-time linear systems subject to disturbances. *Proceedings of European Control Conference (ECC)*, IEEE, 2013; 1156–1161.
- 18. Li H, Shi Y. Event-triggered robust model predictive control of continuous-time nonlinear systems. *Automatica* 2014; **50**(5):1507–1513.
- Sijs J, Lazar M, Heemels W. On integration of event-based estimation and robust MPC in a feedback loop. Proceedings of the 13th ACM international conference on Hybrid systems: computation and control, ACM, 2010; 31–40
- 20. Liu C, Gao J, Li H, Xu D. Aperiodic robust model predictive control for constrained continuous-time nonlinear systems: An event-triggered approach. *IEEE Transactions on Cybernetics* 2017; **48**(5):1397–1405.
- 21. Luo Y, Xia Y, Sun Z. Robust event-triggered model predictive control for constrained linear continuous system. *International Journal of Robust and Nonlinear Control* 2019; **29**(5):1216–1229.
- Berglind JB, Gommans T, Heemels W. Self-triggered MPC for constrained linear systems and quadratic costs. IFAC Proceedings Volumes 2012; 45(17):342–348.
- 23. Brunner FD, Heemels W, Allgöwer F. Robust self-triggered MPC for constrained linear systems. *Proceedings of European Control Conference*, IEEE, 2014; 472–477.
- 24. Eqtami A, Heshmati-alamdari S, Dimarogonas DV, Kyriakopoulos KJ. Self-triggered model predictive control for nonholonomic systems. *Proceedings of 2013 European Control Conference*, IEEE, 2013; 638–643.
- Gommans T, Heemels W. Resource-aware MPC for constrained nonlinear systems: A self-triggered control approach. Systems & Control Letters 2015; 79:59–67.
- 26. Henriksson E, Quevedo DE, Sandberg H, Johansson KH. Self-triggered model predictive control for network scheduling and control1. *Proceedings of the 8th IFAC Symposium on Advanced Control of Chemical Processes* 2012; **45**(15):432–438.
- 27. Yang H, Li Q, Zuo Z, Zhao H. Self-triggered mpc for nonholonomic systems with multiple constraints by adaptive transmission intervals. *Automatica* 2021; **133**:109 870.
- 28. Li A, Sun J. Self-triggered model predictive control for nonlinear continuous-time networked system via ensured performance control samples selection. *International Journal of Control* 2021; (Accepted):1–18.
- 29. He N, Shi D, Chen T. Self-triggered model predictive control for networked control systems based on first-order hold. *International Journal of Robust and Nonlinear Control* 2018; **28**(4):1303–1318.
- 30. Wang X, Yang L. Sporadic model predictive control using Lebesgue approximation. *Proceedings of American Control Conference*, IEEE, 2017; 5768–5773.
- 31. Tao J, Yang L, Wu ZG, Wang X, Su H. Lebesgue approximation model predictive control of nonlinear sampled-data systems. *IEEE Transactions on Automatic Control* 2020; **65**(10):4047–4060.
- 32. Yang L, Wang X. Lebesgue-approximation-based model predictive control for nonlinear sampled-data systems with measurement noises. *Proceedings of American Control Conference*, IEEE, 2018; 3147–3152.
- 33. Limón D, Alamo T, Salas F, Camacho EF. Input to state stability of min-max MPC controllers for nonlinear systems with bounded uncertainties. *Automatica* 2006; **42**(5):797–803.
- 34. Kazantzis N, Kravaris C. Time-discretization of nonlinear control systems via taylor methods. *Computers & Chemical Engineering* 1999; **23**(6):763–784.
- 35. Kvasnica M, Grieder P, Baotić M, Morari M. Multi-parametric toolbox (MPT). *International Workshop on Hybrid Systems: Computation and Control*, Springer, 2004; 448–462.
- 36. Lazar M. Model predictive control of hybrid systems: Stability and robustness. *Dissertation Abstracts International* 2006; **68**(01).
- 37. TøNdel P, Johansen TA, Bemporad A. An algorithm for multi-parametric quadratic programming and explicit mpc solutions. *Automatica* 2003; **39**(3):489–497.
- 38. Houska B, Ferreau HJ, Diehl M. An auto-generated real-time iteration algorithm for nonlinear MPC in the microsecond range. *Automatica* 2011; **47**(10):2279–2285.